Cell Host & Microbe, *Volume 6*

Supplemental Data

Inflammatory Monocytes Facilitate Adaptive CD4 T Cell Responses during Respiratory Fungal Infection

Tobias M. Hohl, Amariliz Rivera, Lauren Lipuma, Alena Gallegos, Chao Shi, Mathias Mack, and Eric G. Pamer

Supplemental Experimental Procedures

Generation of CCR2 Depleter Mice

To generate CCR2 depleter mice, BAC clone RP23-182D4 (CHORI, Oakland, CA) encoding the endogenous CCR2 locus was modified by homologous recombination using the recombineering strategy pioneered by Heintz and colleagues (Gong et al., 2002). The same technique was used to generate CCR2 reporter mice (Serbina et al., 2009). Briefly, the murine CCR2 locus was identified on BAC clone RP23-182D4 by PCR screening of candidate BACs mapped to the distal end of chromosome 9. A 1.7 Kb fragment that contained 1.0 kb upstream and 0.7 kb downstream of the CCR2 gene start codon was amplified and modified between the first and second codon of CCR2 through insertion of nucleotides that encode amino acids 1-208 of African green monkey DTR (GenBank M93012) followed by a 12 residue linker (-GSGGSGGSGGTG-), a 19 residue aphthovirus 2A cleavage site (-APVKQTLNFDLLKLAGDVESNPGP-) (Donnelly et al., 2001) and enhanced cyan fluorescent protein (amino acids 2-239) (Tsien, 1998). The CFP coding sequence was followed by a stop codon and the ensuing nucleotide at position 4 of the

endogenous CCR2 locus was deleted. The resulting 3.2 Kb fragment encoding the DTR-CFP insert was cloned into Asc I and Not I sites in the shuttle vector pLD53SC.AB, kindly obtained from Dr. Daniel Littman (New York University, New York, NY).

The linker sequence between the DTR and the fluorescent protein coding sequences was optimized for fluorescence as described in Fig. S2. Briefly, DTR-GFP constructs encoding the indicated linker sequences between the DTR and GFP modules were assembled by overlap PCR, sequenced, and cloned into the Mlu I and Not I sites of the pCI-neo plasmid (Promega). RAW 264.7 cells were transfected with indicated constructs and analyzed by flow cytometry for fluorescence intensity.

The shuttle vector containing the 3.2 Kb fragment encoding the DTR-CFP insert was integrated into the BAC by homologous recombination and co-integrates were identified by chloramphenicol and ampicillin selection. Resolution of co-integrates through a second homologous recombination event was achieved by negative selection on sucrose, resulting in the complete excision of the shuttle vector backbone that includes the *SacB* gene (for details see (Gong et al., 2002)). The resulting modified BAC encoding DTR-CFP under control of the endogenous CCR2 promoter and regulatory elements was analyzed by Southern blotting to verify CFP integration at the expected site, sequenced over the modified CCR2 gene locus, purified by centrifugation through a cesium chloride gradient, and injected into fertilized C57BL6/J oocytes. Two potential founder animals were identified among 15 offspring screened by PCR and flow cytometric analysis of peripheral blood

samples. Germline transmission was observed in one of two candidate CCR2 depleter founders.

CCR2 depleter mice were crossed to $CX_3CR_1^{(gfp/gfp)}$ "knock-in" mice (Jung et al., 2000) to generate progeny that encode fluorescent transgenes under control of the CX_3CR_1 (GFP) and CCR2 (CFP) promoters. CCR2 reporter mice were crossed with C57BL/6.SJL mice (Jackson Labs) to generate $CD45.1^+CD45.2^+$ CCR2 reporters for adoptive transfer experiments.

Antibodies for Flow Cytometry

All antibodies were purchased from BD Biosciences unless stated otherwise. The staining protocols included combinations of the following antibodies: anti-Ly6C (clone AL-21, FITC or Alexa 700 conjugate), anti-Ly6G (1A8, PE), anti-CD11b (M1/70, PerCP-Cy5.5), anti-CD11c (HL3, APC or PE-Cy7), anti-CD103 (OX62, PE; eBioscience), anti-7/4 (7/4, Alexa 700; AbD Serotec), anti-CD45 (30F-11; APC-Cy7), anti-CD45.1 (A20, APC-Cy7), anti-CD45.2 (104, Alexa 700; eBioscience), anti-MHC class II (M5/114.15.2; PE or Alexa 700; eBioscience), anti-CD8a (53-6.7, PE), anti-CD4 (GK1.5, APC-Alexa Fluor 750), anti-CD90.1 (OX-7, PerCP), anti-CD90.2 (53-2.1, APC), and anti-HB-EGF (biotinylated anti-DTR; R&D Systems, Cat. No. BAF259). The anti-Ly6C-Alexa 700 conjugate was generated in-house at the MSKCC monoclonal Ab core facility. The CCR2 mAb (clone MC-21) (Mack et al., 2001) was used at 5 mg/ml to bind to cells blocked with 4 μg/ml mouse anti-mouse anti-CD16.2/anti-CD32.2 (). CCR2 staining was visualized by staining cells sequentially with 0.1 μg/ml biotinylated anti-rat IgG_{2b} (AbD Serotec) and 0.5 μg/ml APC-linked strepavidin

together with conjugated antibodies.

For intracellular cytokine staining, splenic APCs were loaded with hyphal antigens overnight prior to addition of BAL cells. Cultures were incubated for 5 h in the presence of GolgiPlug (BD Biosciences) prior to processing for intracellular cytokine staining as described in (Rivera et al., 2005).

Generation of Bone Marrow Chimeric Mice

C57BL/6 mice were irradiated with 950 cGy and infused with 2 x 10^6 CD45.1/CD45.2 bone marrow cells from CCR2 depleter mice on the following day. The mice were treated with enrofloxacin in the drinking water to prevent bacterial infections and rested for eight weeks prior to use in experiments.

Supplemental References

Donnelly, M.L., Hughes, L.E., Luke, G., Mendoza, H., ten Dam, E., Gani, D., and Ryan, M.D. (2001). The 'cleavage' activities of foot-and-mouth disease virus 2A site-directed mutants and naturally occurring '2A-like' sequences. The Journal of General Virology *82*, 1027-1041.

Gong, S., Yang, X.W., Li, C., and Heintz, N. (2002). Highly efficient modification of bacterial artificial chromosomes (BACs) using novel shuttle vectors containing the R6Kgamma origin of replication. Genome Res *12*, 1992-1998.

Jung, S., Aliberti, J., Graemmel, P., Sunshine, M.J., Kreutzberg, G.W., Sher, A., and Littman, D.R. (2000). Analysis of fractalkine receptor CX(3)CR1 function by targeted deletion and green fluorescent protein reporter gene insertion. Mol Cell Biol *20*, 4106-4114.

Jung, S., Unutmaz, D., Wong, P., Sano, G., De los Santos, K., Sparwasser, T., Wu, S., Vuthoori, S., Ko, K., Zavala, F.*, et al.* (2002). In vivo depletion of CD11c(+) dendritic cells abrogates priming of CD8(+) T cells by exogenous cell-associated antigens. Immunity *17*, 211-220.

Mack, M., Cihak, J., Simonis, C., Luckow, B., Proudfoot, A.E., Plachy, J., Bruhl, H., Frink, M., Anders, H.J., Vielhauer, V.*, et al.* (2001). Expression and characterization of the chemokine receptors CCR2 and CCR5 in mice. J Immunol *166*, 4697-4704.

Rivera, A., Van Epps, H.L., Hohl, T.M., Rizzuto, G., and Pamer, E.G. (2005). Distinct CD4+-T-cell responses to live and heat-inactivated Aspergillus fumigatus conidia. Infect Immun *73*, 7170-7179.

Serbina, N.V., Hohl, T.M., Cherny, M., and Pamer, E.G. (2009). Selective expansion of the monocytic lineage directed by bacterial infection. J Immunol *183*, 1900-1910.

Tsien, R.Y. (1998). The green fluorescent protein. Annu Rev Biochem *67*, 509-544.

Supplemental Figures

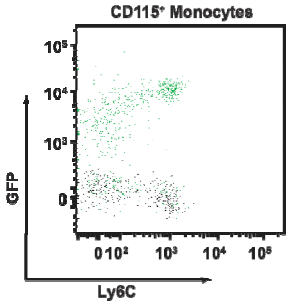

Figure S1. *GFP Expression by Circulating Monocytes in CCR2 Reporter Mice*

Ly6C^{hi} monocytes express higher GFP transgene levels than Ly6C^{lo} monocytes. The plot shows GFP and Ly6C expression by CD115^{+} blood monocytes isolated from a CCR2 reporter mouse (green dots) or a non-transgenic C57BL/6 littermate (black dots).

A

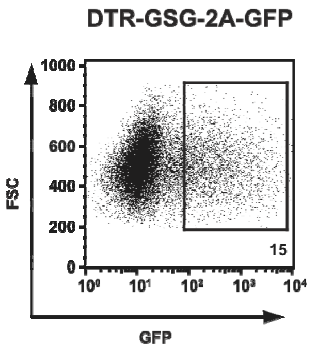

B

CONSTRUCT	LINKER SEQUENCE	MFI
GFP	Not applicable	2,839
DTR-GFP	-HPDPPVA-	734
DTR-GSG-GFP	$-(GSG)_3GTG-$	510
DTR-2A-GFP	-GSG-2A-	735
DTR-GSG-2A-GFP	$-(GSG)_3GTG-2A-$	995

Figure S2. *Optimization of Linker Sequence between DTR and Fluorescent Protein Coding Sequences*

(A) Flow cytometric analysis of RAW264.7 cells transfected with a pCI-neo plasmid construct that encodes a DTR-GSG-2A-GFP gene. The plot is gated on live cells 24 h post-transfection with forward scatter on the ordinate and GFP expression on the abscissa. (B) The table shows a comparison of the mean fluorescence intensity (MFI) of GFP^+ cells (see gate in panel A) of RAW 264.7 cells transfected with the indicated constructs. The 19 residue 2A cleavage site consists of the sequence -APVKQTLNFDLLKLAGDVESNPGP-. The DTR-GFP linker sequence is derived from (Jung et al., 2002).

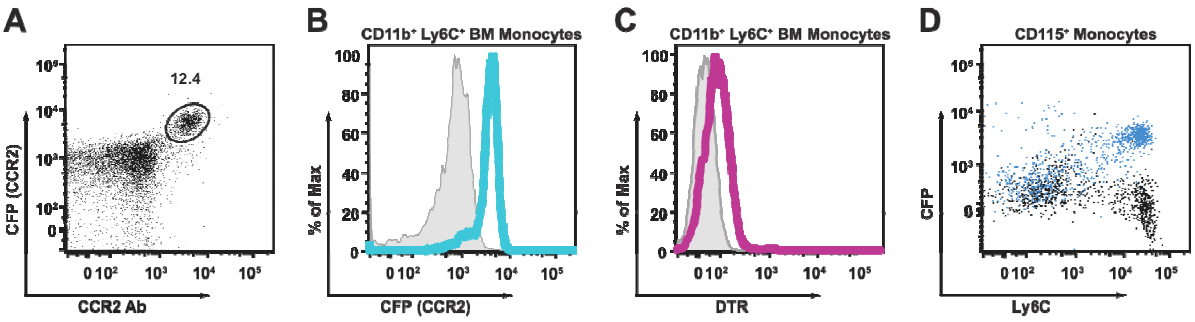

Figure S3. *Characterization of CCR2 Depleter Mice*

(A) Transgene expression recapitulates CCR2 expression. The plot shows CFP expression by bone marrow cells on the ordinate with CCR2 Ab surface staining on the abcissa. (B, C) CD11b^{+}Ly6C^{hi} bone marrow monocytes from CCR2 depleter mice were analyzed for (B) CFP (cyan line) and (C) DTR (pink line) expression. The background fluorescence signal from non-transgenic mice (B) and isotype control staining (C) is shown in the grey histograms. (D) The plot shows CFP and Ly6C expression by CD115^{+} blood monocytes isolated from a CCR2 depleter mouse (blue dots) or a non-transgenic C57BL/6 mouse (black dots).

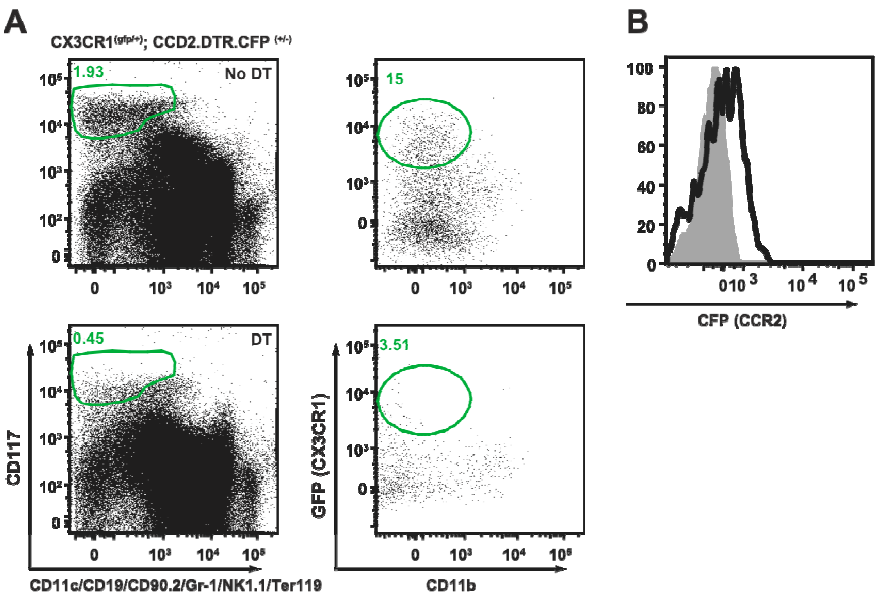

Figure S4. *Toxin-Mediated Ablation of MDPs*

(A) DT administration leads to MDP depletion in mice that express a GFP transgene at the CX_3CR_1 locus and CFP and DTR transgenes under control of the CCR2 promoter ($CX_3CR_1^{(gfp/+)}$ CCR2 depleter mice). Littermates were treated with no DT (top row) or 10 ng/gram body weight DT (bottom row) and bone marrow cells were analyzed by flow cytometry 24 h after DT administration. The plots in the bottom row show a ~75% reduction in the frequency of CD117+Lin- cells (green gate, left column). CD117+Lin- cells were further analyzed for GFP (CX3CR1) and CD11b expression and MDPs are indicated in the oval-shaped green gate (middle column). (B) MDPs express low levels of the CFP transgene. The histogram shows CFP (CCR2) fluorescence from MDPs gated according to the strategy in (A) from $CX_3CR_1^{(gfp/+)}$ CCR2 depleter mice (black line)or $CX_3CR_1^{(gfp/+)}$ littermates (filled grey line).

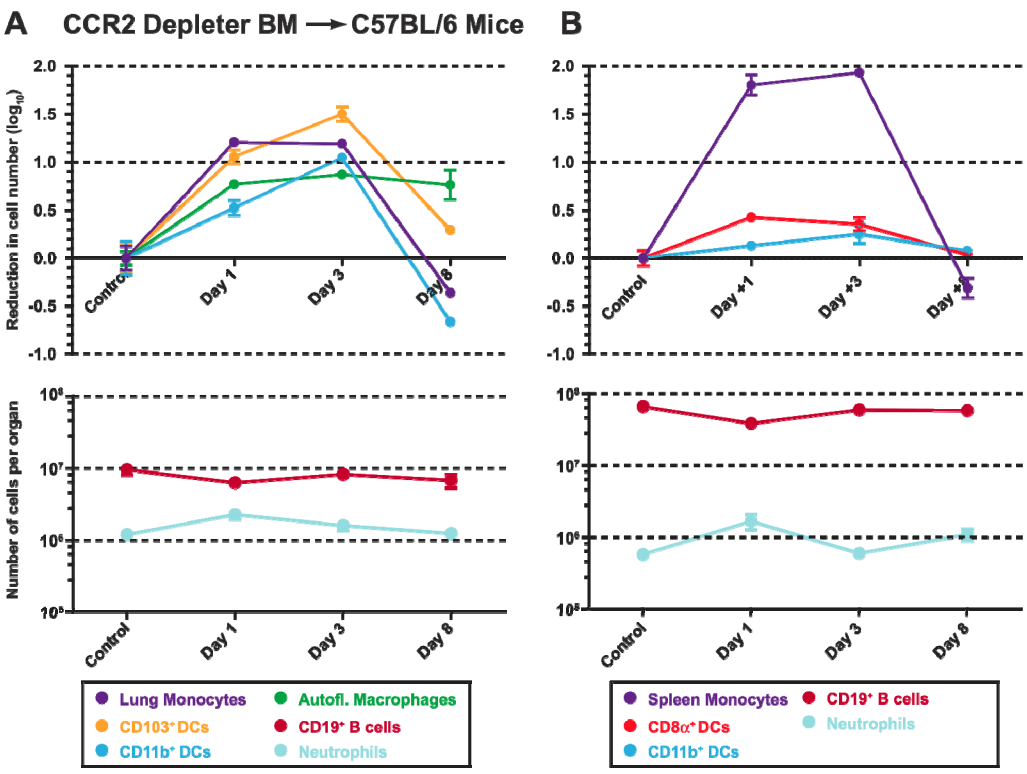

Figure S5. *Depletion of Lung and Spleen DC Subsets in Bone Marrow Chimeric Mice*

(A-B) Irradiated C57BL/6 mice were reconstituted with CCR2 depleter bone marrow cells and rested for 8 weeks prior to DT (10 ng/gram body weight) or no DT (controls) administration on day 0. At indicated time points, mice were euthanized and single cell lung (A) and spleen (B) suspensions were enumerated and analyzed by flow cytometry to determine toxin-induced cell depletion.

For the top panel in (A), the baseline lung monocyte, CD103$^+$ DC, CD11b$^+$ DC, and lung macrophage counts (± SEM) were (in log10 units) 6.293±5.631, 5.591±5.055, 5.879±5.388, and 6.033±5.261, respectively. For the top panel in (B), the baseline spleen monocyte, CD8α$^+$ DC, and CD11b$^+$ DC counts (±SEM) were 5.913±4.707, 5.463±4.778, and 6.009±4.683, respectively.

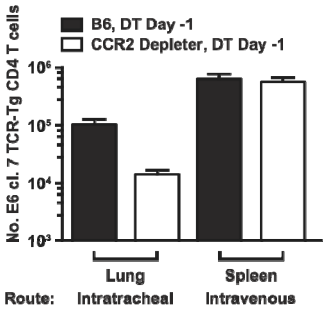

Figure S6. *Compartment-Specific CD4 T Cell Expansion in CCR2 Depleter Mice following Intratracheal or Intravenous Challenge with ActA- Listeria Monocytogenes*

The bar graph shows the number (±SEM, n=3-4/group) of ESAT-6-specific clone 7 TCR-Tg CD4 T cells in the lungs and spleen of CCR2 depleter (black columns) or control mice (white columns) 6 days post-challenge with ESAT-6-expressing ActA$^-$ *L. monocytogenes* (A. Gallegos et al., manuscript in preparation) via the i.t. (10^5 inoculum) or i.v. route (2 x 10^3 inoculum), respectively. All mice received10^4 ESAT-6-specific clone 7 TCR-Tg CD4 T cells via the lateral tail vein 2 days prior to infection and a single 10 ng/gram body weight DT injection one day prior to infection.